UC Davis
UC Davis Previously Published Works

Title

Oxidative damage to rhesus macaque spermatozoa results in mitotic arrest and transcript abundance changes in early embryos.

Permalink

https://escholarship.org/uc/item/95p707th

Journal

Biology of reproduction, 89(3)

ISSN

0006-3363

Authors

Burruel, Victoria
Klooster, Katie L
Chitwood, James
et al.

Publication Date

2013-09-01

DOI

10.1095/biolreprod.113.110981

Peer reviewed

Oxidative Damage to Rhesus Macaque Spermatozoa Results in Mitotic Arrest and Transcript Abundance Changes in Early Embryos[1]

Victoria Burruel,[3] Katie L. Klooster,[3] James Chitwood,[4] Pablo J. Ross,[4] and Stuart A. Meyers[2,3]

[3]Department of Anatomy, Physiology, and Cell Biology, School of Veterinary Medicine, University of California Davis, Davis, California
[4]Department of Animal Science, University of California Davis, Davis, California

ABSTRACT

Our objective was to determine whether oxidative damage of rhesus macaque sperm induced by reactive oxygen species (ROS) in vitro would affect embryo development following intracytoplasmic sperm injection (ICSI) of metaphase II (MII) oocytes. Fresh rhesus macaque spermatozoa were treated with ROS as follows: 1 mM xanthine and 0.1 U/ml xanthine oxidase (XXO) at 37°C and 5% CO_2 in air for 2.25 h. Sperm were then assessed for motility, viability, and lipid peroxidation. Motile ROS-treated and control sperm were used for ICSI of MII oocytes. Embryo culture was evaluated for 3 days for development to the eight-cell stage. Embryos were fixed and stained for signs of cytoplasmic and nuclear abnormalities. Gene expression was analyzed by RNA-Seq in two-cell embryos from control and treated groups. Exposure of sperm to XXO resulted in increased lipid peroxidation and decreased sperm motility. ICSI of MII oocytes with motile sperm induced similar rates of fertilization and cleavage between treatments. Development to four- and eight-cell stage was significantly lower for embryos generated with ROS-treated sperm than for controls. All embryos produced from ROS-treated sperm demonstrated permanent embryonic arrest and varying degrees of degeneration and nuclear fragmentation, changes that are suggestive of prolonged senescence or apoptotic cell death. RNA-Seq analysis of two-cell embryos showed changes in transcript abundance resulting from sperm treatment with ROS. Differentially expressed genes were enriched for processes associated with cytoskeletal organization, cell adhesion, and protein phosphorylation. ROS-induced damage to sperm adversely affects embryo development by contributing to mitotic arrest after ICSI of MII rhesus oocytes. Changes in transcript abundance in embryos destined for mitotic arrest is evident at the two-cell stage of development.

early development, embryo development, fertilization, gene expression, oxidative stress, sperm

INTRODUCTION

Cryopreservation induces a severe osmotic insult to the cell that leads to generation of reactive oxygen species (ROS) including superoxide anion, hydrogen peroxide, hydroxyl radical, and singlet oxygen [1–4]. This process can be minimized but not eliminated by using cryopreservative agents. There is substantial evidence that sperm cryopreservation results in increased DNA damage, aneuploidy, and chromosome fragmentation as well as specific sublethal effects like chromatin cross-linking, base changes, and DNA strand breaks [5–8]. A limited ability to store antioxidant enzymes combined with a membrane rich in unsaturated fatty acids makes spermatozoa particularly susceptible to oxidative stress and peroxidative attack by ROS, specifically superoxide anion and hydrogen peroxide [9]. Low to high levels of ROS have been associated with extensive sperm damage, including morphological defects [10], lipid peroxidation and DNA fragmentation [11], decreased ability of the acrosome to react or fuse with the oocyte [12], and compromised pregnancy after in vitro fertilization [13, 14]. There is clinical evidence that damage to sperm DNA impairs both embryo development and pregnancy in mice and humans [15–18]. High levels of ROS have been associated with sperm DNA damage in the semen of 25% of infertile men [19] and recent evidence indicates that partners of men with high DNA fragmentation indices have significantly higher rates of spontaneous abortion [20]. An increase in abnormal sperm morphology is correlated with higher seminal ROS levels [21–23] than morphologically normal sperm. High concentrations of leukocytes seen with infections such as epididymitis and chronic prostatitis are known to increase ROS levels in semen [24, 25] and contribute to infertility. Although cryopreservation of ejaculated sperm has been in clinical and agricultural use for decades, it remains unclear how sperm damage as a result of cryopreservation contributes to embryonic or fetal loss.

Embryo development is characterized by cell division accompanied by a number of distinct biological processes that are controlled by genes that are activated differentially at varying stages of development [26, 27]. Following fertilization, the embryonic genome activates during the first days postfertilization as cell division progresses. Most mRNA is supplied by the oocyte and then augmented and replaced by mRNA from stage-specific and species-specific embryonic genome activation (EGA). In human embryos, paternal transcripts are first observed at the three- to four-cell stage and protein synthesis linked to transcriptional activation is evident around the four- to eight-cell stage [28, 29]. Rhesus EGA reportedly occurs around the six- to eight-cell cleavage stage [30, 31]. In the bovine eight-cell embryo, it was reported that 258 genes were upregulated as compared to metaphase II (MII) bovine oocytes [32]. These authors also noted that in vitro-produced embryos are known to have different mRNA

expression patterns compared to in vivo-derived cohorts, probably reflecting the sensitivity of EGA to culture conditions. Events that occur during the preimplantation embryo phase are highly likely to be essential for later development of the conceptus and placenta. It has been estimated that fewer than 50% of all in vitro-fertilized embryos reach the blastocyst stage of development because of suboptimal environment during culture with subsequent pregnancy rates of 26%–30% [33, 34]. Further, 50%–80% of human embryos in the first two cleavages have been reported to carry abnormal chromosome numbers demonstrating aneuploidy [35]. Human aneuploidies have been associated with oocyte aging; however, male-factor infertility has been associated with women of a variety of ages. The role of direct sperm effects on EGA has not been reported for any species.

Our laboratory has demonstrated that cryopreserved rhesus sperm undergoes oxidative stress resulting in increased levels of lipid peroxidation, decreased motility, and cytoskeletal rearrangement in response to cryopreservation [36–38]. We hypothesize that a primary mechanism for embryo mortality may be cryopreservation-induced oxidative stress in fertilization-capable sperm. In an effort to further understand how sperm can contribute to embryonic loss, we microinjected live motile sperm that had been experimentally exposed to ROS as a model for cryopreservation-induced damage in order to determine the downstream effects on embryo development.

MATERIALS AND METHODS

Reagents/Chemicals

The fluorochromes C_{11}-BODIPY (4,4-difluro-5-(4-phenyl-1,3-butadienyl)-4-bora-3a,4a-diaza-s-indacene-3-undecanoic acid) and propidium iodide (PI) were obtained from Invitrogen. Chemicals were obtained from Sigma Chemical Co. unless otherwise stated.

Experimental Design

Experiment 1. Ejaculated sperm from four rhesus males were incubated for 135 min, during which ROS were induced by xanthine-xanthine oxidase (XXO) exposure or control vehicle only. Mature (MII) oocytes (n = 96) from four superovulated rhesus females were randomly assigned to be injected by sperm exposed to control (n = 53) or XXO (n = 43) treatment and sperm were selected for intracytoplasmic sperm injection (ICSI). Embryos were then incubated and visually assessed at 12-h intervals for quality and stage of development.

Experiment 2. Treatments were as described for Experiment 1; however, control embryos were harvested at first detection of two-, four-, and eight-cell stages for fluorescence labeling of nuclear integrity and mitotic spindle and tubulin network assessment (n = 13). In addition, seven control embryos and four XXO-treated embryos at the four-cell stage were harvested for RNA-Seq analysis. Embryos from the XXO treatment group that were arrested at the two- or four-cell stage were harvested (n = 17) after control embryos progressed and when it was evident they were not undergoing cell division to the subsequent stage.

Sperm Preparation

Animals were housed at California National Primate Research Center and maintained according to Institutional Animal Care and Use Committee protocols at the University of California. All guidelines suggested by *Biology of Reproduction* were followed for the highest possible standards for the humane care and use of animals in research. Semen samples were obtained by electroejaculation from four male rhesus macaques (*Macaca mulatta*) as previously described [39]. Semen samples were collected directly into 50-ml centrifuge tubes containing 5 ml of HEPES-Biggers, Whitten, and Whittingham (BWW) media. Following semen collection, the coagulum was removed and samples were centrifuged down to a pellet for 8 min. The pellet was diluted in 5 ml HEPES-BWW containing 1 mg/ml polyvinylalcohol (PVA) and motility and forward progression recorded. Two and a half milliliters of diluted semen was layered over 3 ml of 80% buffered Percoll and centrifuged at $300 \times g$ for 25 min as previously described [40, 41]. Following centrifugation, the

supernatant was removed, the pellet was washed twice in HEPES-BWW with 1 mg/ml PVA ($300 \times g$, 5 min), and spermatozoa were resuspended in BWW with 1 mg/ml PVA to a final concentration of 25×10^6/ml in 500-μl aliquots.

Induction of ROS in Sperm

An XXO ROS-producing system was used to induce ROS production in rhesus monkey sperm as previously reported [36, 42, 43]. The XXO system primarily results in generation of superoxide anion and hydrogen peroxide. Sperm at a concentration of 25×10^6/ml were incubated for 135 min (T_{135}) with or without 1 mM xanthine and 1 mM xanthine oxidase at 37°C, 5% CO_2 in air. Sperm motility was evaluated at 0 (T_0) and 135 min (T_{135}), and sperm were processed for determination of viability and lipid peroxidation. The lipid peroxidase promoters ferrous sulfate (1 μM) and sodium ascorbate (5 μM) were added to both treatments. Sperm were washed in BWW and centrifuged for 3 min at $300 \times g$. Sperm selected for ICSI were further diluted with BWW containing 1 mg/ml PVA to a final sperm concentration of 4×10^6/ml.

Motility

Sperm total and progressive motility were evaluated by means of computer-assisted sperm analysis (CASA) with HTM Ceros, version 14 (Hamilton Thorne Biosciences, Inc.). At least 200 cells in a minimum of four fields were evaluated for each treatment. The following instrument settings were used for CASA analysis for rhesus sperm: frame rate, 60 Hz; frames acquired, 30; minimum contrast, 80; minimum cell size, four pixels; static average path velocity (VAP) cutoff, 20 μ/sec; static straight-line (rectilinear) velocity (VSL) cutoff, 10 μ/sec; progressive VAP threshold, 25 μ/sec; progressive straightness (STR) threshold, 80%; static intensity limits, 0.6–1.4; static size limits, 0.6–2.31; and static elongation limits, 0–80. Because ROS-treated sperm lost significant motility after treatment, we also analyzed posttreatment motility using manual motility and forward progression assessment [44]. A 10-μl drop of sperm suspension was placed on a slide and a coverslip placed over it. A minimum of 200 sperm were counted per slide and triplicate aliquots were counted for total and forward progression.

Detection of Sperm Lipid Peroxidation

The fluorescence lipid probe C_{11}-BODIPY was used to assess lipid peroxidation as previously reported [36]. When C_{11}-BODIPY becomes incorporated into the sperm membrane, it fluoresces red until lipid radicals peroxidize the membrane, at which time the probe undergoes an emission shift to green (red, nonperoxidized; green, peroxidized). Spermatozoa were incubated in 1 μM C_{11}-BODIPY for 30 min at room temperature to load the probe into the cell membranes prior to treatment. Spermatozoa were then washed two times at $300 \times g$ for 5 min to remove excess probe and resuspended to 25×10^6 sperm/ml in their respective treatments in the presence or absence of the lipid peroxidation promoters ferrous sulfate (1 μM) and sodium ascorbate (5 μM). Because nonviable cells may undergo lipid peroxidation, the vitality probe PI (final concentration 12 μM) was added during the last 5 min of treatment incubation so that nonviable lipid-peroxidized cells could be distinguished from live lipid-peroxidized cells using the flow cytometer. Viability was determined by the percentage of PI-negative cells. Spermatozoa were then diluted to 1×10^6 sperm/ml and analyzed by flow cytometry. Flow cytometry was performed using a FACScan cytometer (Becton-Dickinson) equipped with a 488-nm excitation laser and data were analyzed using CellQuest software (Becton-Dickinson). PI and C_{11}-BODIPY fluorescence was measured using 585/42 and 581/591 (excitation/emission) band-pass filters, respectively. Adjustments were made to address and eliminate fluorochrome spectral overlap so that each cell population was seen as distinct. In order to limit the evaluation of C_{11}-BODIPY fluorescence to viable spermatozoa, only the subpopulation outside of PI-positive cells was included in the evaluation. A total of 10 000 gated events were analyzed per sample.

Superovulation, Oocyte Collection, and ICSI

Females with a history of regular menstrual cycles scheduled for necropsy were selected as oocyte donors for superovulation and oocyte collection. Beginning on Days 1–4 of menses, females were superovulated with injections of the gonadotropin-releasing hormone antagonist Acyline (60 μg/kg/day, s.c.) for 8 consecutive days, with concurrent injections of recombinant human follicle stimulation hormone (rhFSH, 30 IU i.m. twice daily; Follistim; Merck). Injections of recombinant human luteinizing hormone (30 IU s.c. injections twice daily; Luveris; EMD Serono) were given on the last 2 days of rhFSH and antagonist treatment. A single injection of human chorionic gonadotropin (1300 IU i.m.; Ovidrel; EMD Serono) was given 35 h before follicular aspiration. At
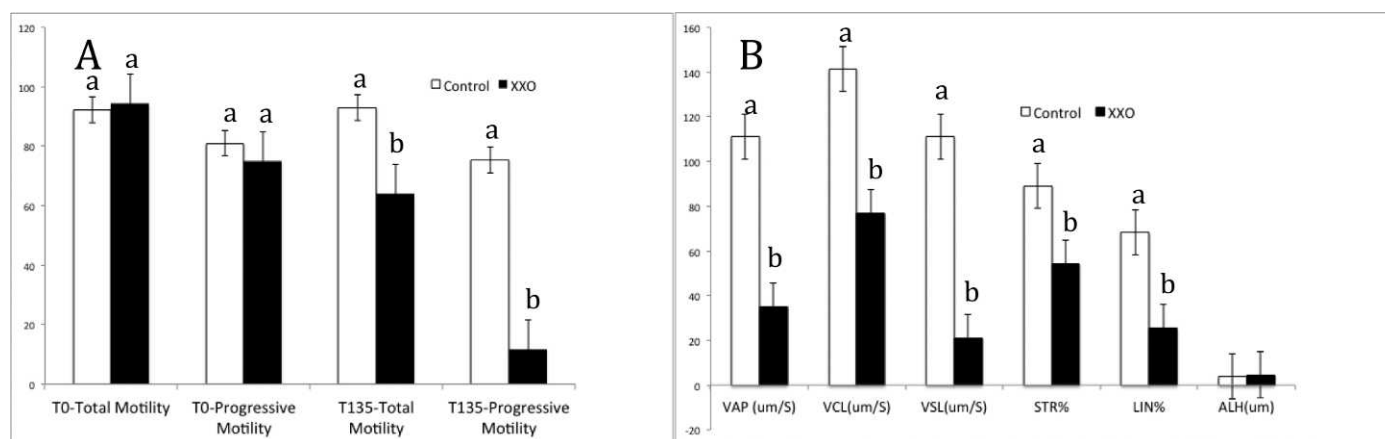
FIG. 1. **A**) Total and progressive motility at the beginning (T0) and end of XXO treatment (T135). Progressive motility in the XXO group was significantly different from that of controls. **B**) Sperm motility parameters for sperm selected for ICSI from control and XXO-treated spermatozoa: VAP (μm/sec); VCL, curvilinear velocity (μm/sec); VSL (μm/sec); STR; LIN, linearity; ALH, amplitude of lateral head displacement (μm or Hz). Different superscripts indicate significant differences ($P < 0.05$).

necropsy, follicles of the excised ovaries were punctured using a 1.5-inch, 20-gauge needle attached to mild vacuum pressure into 15-ml sterile tissue culture tubes of Tyrode albumin lactate pyruvate medium buffered with HEPES at 37°C and immediately transported to the laboratory for recovery of oocytes at 37°C. Embryos were produced by ICSI of MII oocytes as described previously [45–47] using XXO-treated and control sperm. Only visibly motile sperm observed as having slow-beating tails were chosen for injection for the XXO-treated sperm. Motile sperm with progressive motility were chosen for injection from the control sperm sample. Injected oocytes were cultured in 25-μl drops of HECM-9 [48] under oil (Ovoil; VitroLife) and cultured at 37°C in 6% CO_2, 5% O_2, and 89% N_2.

Embryo Evaluation

Fertilization was determined by visualization of two pronuclei (PN) and extrusion of a second polar body in injected oocytes at 16 h post-ICSI. Zygotes were individually cultured in HECM-9 up to the eight-cell stage. Embryos were cultured individually and observed daily for normal cleavage rates and graded for observation by degree of blastomere fragmentation and asymmetry. Embryos were graded as follows: grade A, less than 10% visible fragmentation and symmetrical blastomeres; grade B, 10%–25% visible fragmentation and symmetrical blastomeres; grade C, greater than 25% fragmentation with asymmetrical blastomeres; and grade D, greater than 50% fragmentation and asymmetrical blastomeres; data not shown [49, 50].

Fluorescence Labeling of Embryos

Embryos were fixed in a 2% paraformaldehyde PIPES buffer with 0.5% Triton X-100 and incubated for 30 min at 37°C. The embryos were washed twice in 0.5 ml of blocking solution (PBS with 5% bovine serum albumin, 0.5% fetal bovine serum, 62.4 μM glycine, and 0.01% Triton X-100) and transferred to 0.5 ml of blocking solution and incubated for 1 h. Embryos were then incubated individually in 10-μl drops with monoclonal anti-α-tubulin-FITC antibody produced in mouse (F2168; Sigma) diluted in Dulbecco PBS (1:100), with 0.3 ml of mineral oil covering the drops at 37°C for 1 h. After two washes in 0.5 ml blocking solution, embryos were incubated for 10 min in 0.4 ml of 10 μM of Hoescht 3342. After staining, embryos were then mounted on a slide with 13 μl of Prolong Gold antifade reagent (P36930; Invitrogen) and a coverslip was gently placed to cover the embryo. The Prolong was allowed to cure overnight at room temperature before embryos were imaged.

Embryos were imaged at 40× magnification using a Zeiss fluorescence microscope (AxioImager AX10) equipped with an X-Cite Series 120 lamp and motor-driven stage for z-series sequences. Zeiss AxioVision (Release 4.7.1; Carl Zeiss, Inc.) software was used for multichannel and z-series photos.

RNA Sequencing

Embryos at the two-cell stage from control (n = 7) and XXO treatment (n = 4) were placed in Extraction Buffer (Arcturus PicoPure RNA Isolation kit; Invitrogen), snap frozen in LN2, and stored at −80°C until RNA isolation. RNA from two embryos in each treatment was isolated using the Arcturus Picopure RNA isolation kit including DNAse treatment as indicated by the manufacturer. The RNA was eluted in a total of 7 μl of water. Two microliters was used to corroborate RNA quantity and quality on an Experion high-sensitivity RNA chip (Bio-Rad). Then, 400 pg of total RNA was converted to cDNA and the cDNA amplified by a SPIA approach using the Ovation RNA-Seq kit from Nugen [51]. Finally, the amplified cDNA was used to generate a sequencing library using the Encore NGS Library preparation kit (Nugen). The library was submitted to the UC Davis Genome Center for quality control, quantification, and sequencing by a single 40-bp run in the Illumina Genome Analyzer IIx. Bioinformatic analysis was performed using CLC Genomics Workbench (CLC bio). High-quality reads were mapped to the annotated *M. mulatta* genome sequence with annotation using the RNA-Seq algorithm from CLC Genomics Workbench. Reference sequences were obtained from ENSEMBL. Statistical analysis of gene expression levels was performed using DESeq with total exon read counts as input data [52]. Gene ontology functional annotation was performed using the Database for Annotation, Visualization, and Integrated Discovery (DAVID) [53, 54].

Statistical Analysis

Comparisons of sperm lipid peroxidation and viability were performed using one-way ANOVA techniques with Minitab statistical software (Minitab Inc.). Data are expressed as the mean ± SEM. Embryo data for the number of four-cell embryos that cleaved to the eight-cell stage was analyzed using logistic regression analysis (SAS).

RESULTS

Sperm Characteristics after ROS Treatment

The percentages of motile sperm, viable sperm, and sperm with high levels of lipid peroxidation were determined at the end of the 135-min incubation period (T_{135}). Initial total and progressive motility for the control and XXO sperm (Fig. 1A) were not different between groups ($P > 0.05$). The mean percentages of total and progressive motility differed at T_{135} for control and XXO sperm. Motility assessment revealed that the majority of sperm were weakly motile (64% total motility) after XXO treatment and demonstrated poor progressive motility (Fig. 1, A and B). Analysis of individual sperm tracks revealed that all motility parameters were diminished in XXO-treated sperm (Fig. 1B). Overall, these results suggest that XXO treatment reduces sperm motility, with specific impact on progressive motility. The mean percentage of viable sperm (Fig. 2) in the control and XXO groups were 92.2% ± 2% and 93.8% ± 1%, respectively ($P > 0.05$), indicating that sperm with poor motility retained membrane integrity and cell viability. The percentages of viable sperm and sperm with
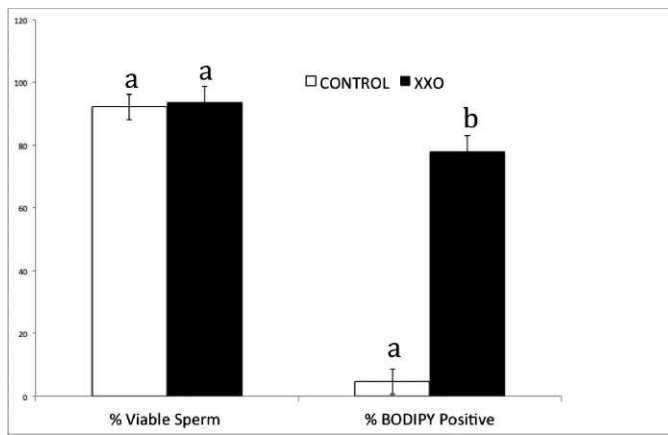
Article 72

FIG. 2. Mean percentages of viable sperm and high membrane lipid peroxidation of sperm injected into oocytes. Viable sperm was determined as the percentage of PI-negative sperm in the samples. The percentage of lipid peroxidation was determined as the percentage of C_{11}-BODIPY-positively labeled sperm. Different superscripts indicate significant differences ($P < 0.05$).

high levels of lipid peroxidation were determined at T_{135} and the mean percentages of high-lipid-peroxidation sperm in the control and XXO group were different at T_{135} ($P < 0.05$). In the control group, less than 5% of sperm demonstrated any lipid peroxidation, whereas the majority of sperm in the XXO treatment group displayed high levels of membrane lipid peroxidation.

Development and Morphological Characteristics of Embryos Produced with ROS-Treated Sperm

ICSI was performed using XXO-treated motile rhesus sperm and MII oocytes obtained from superovulated rhesus females. MII oocytes were randomly injected with control or XXO-treated sperm (Table 1 and Fig. 3). The outcomes of fertilization, cleavage on Day 2, number of four-cell embryos on Day 2, and number of eight-cell embryos developed by Day 3 were compared between treatment and control groups through Day 3 of development. The percentage of oocytes fertilized (two PN) and total number of cleaved embryos were not significantly different between sperm treatment groups ($P > 0.05$; Table 1). Control embryos exhibited two PN when assessed at 16 h post-ICSI (83% ± 1%), cleavage to two-cell embryos by 24 h post-ICSI (86% ± 1%), four cells by Day 2

(79% ± 1%), and eight cells by Day 3 (80% ± 1%). Examples of normal developing rhesus embryos are shown in Figure 4, and arrested and fragmented two- to four-cell embryos are displayed in Figure 5. All XXO sperm-treated embryos demonstrated permanent embryonic arrest or varying degrees of degeneration and cytoplasmic and nuclear fragmentation. Exposure of sperm to XXO treatment for 135 min prior to ICSI fertilization resulted in only 1 of 43 embryos developing beyond the four-cell stage, although pronuclear and two-cell stages occurred at the same time points as that of control embryos (Fig. 5).

The percentage of four-cell embryos on Day 2 was 79.0% for controls and 48.0% for the treatment group. The percentage of eight-cell embryos on Day 3 was significantly different between groups with 80.0% for controls and 8.3% for treatment embryos ($P < 0.0001$). These data indicate that exposing sperm to high levels of oxidative stress results in embryos arresting before the eight-cell stage. A control eight-cell embryo is displayed in Figure 6 after fixation and labeling with α-tubulin and DAPI. In this representative embryo, all blastomeres are equivalent and uniform in size and shape, and the nuclei are similarly homogeneous in size and shape. The majority of XXO sperm-treated embryos also exhibited asymmetrical and multinucleated blastomeres, beginning with arrested two-cell embryos and continuing through successive cleavages. Some embryos had multinucleated blastomeres visible from the two-cell to four-cell stage. However, embryos in the treatment group were mainly graded as grades C and D (data not shown), indicating severe fragmentation and asymmetry. Embryos in the control group were mainly graded as grades A and B. Fluorescence labeling of embryos demonstrated that nuclear fragments, which have been termed micronuclei, contain DNA (Figs. 6–8). Figure 6 demonstrates fluorescence labeling of an eight-cell embryo from the control sperm group, and uniform blastomere shape and size, intact and well-defined nuclei, and uniform distribution of α-tubulin microfilaments are observed. In Figure 7, brightfield and fluorescence-labeled four-cell embryos that were fertilized with XXO-treated sperm are shown that were fixed during mitotic arrest. These embryos typically demonstrated cellular fragmentation of blastomeres and we frequently observed nuclei with substantial fragmentation (arrow, Fig. 7d) in addition to the small cellular fragments containing DNA. Occasional abnormal mitotic spindles were observed, and Figure 8a demonstrates a mitotic figure with numerous DNA seeding points, likely from fragmented nuclear material. The large arrow depicts fragmenting DNA associated with a polar body.

TABLE 1. Development of embryos produced by ICSI using control and treated sperm through Day 3 of in vitro culture.*

Treatment group (female)	No. of oocytes injected	No. of fertilized oocytes at 16 h post-ICSI (%)	No. of embryos cleaved at 24 h post-ICSI (%)	No. of 4-cell embryos at Day 2 post-ICSI (%)	No. of 8-cell embryos at Day 3 post-ICSI (%)
Control					
1	11	8 (73%)	5 (62.5%)	5 (100%)	5 (100%)
2	21	16 (76%)	15 (94%)	13 (87%)	11 (85%)
3	8	7 (87.5%)	7 (100%)	5 (71%)	3 (60%)
4	13	13 (100%)	11 (85%)	7 (64%)	5 (71%)
Total (%)	53	44 (83% ± 1%)[a]	38 (86% ± 1%)[a]	30 (79% ± 1%)[a]	24 (80 ± 1%)[a]
XXO					
1	11	6 (54.5%)	5 (83%)	5 (100%)	0 (0%)
2	14	10 (71%)	10 (100%)	5 (50%)	0 (0%)
3	8	7 (87.5%)	7 (100%)	2 (29%)	1 (50%)
4	10	10 (100%)	3 (30%)	0 (0%)	0 (0%)
Total (%)	43	33 (77% ± 1%)[a]	25 (76% ± 1%)[a]	12 (48% ± 1%)[b]	1 (8% ± 1%)[b]

* Embryos were cultured in serum-free HECM-9 until Day 3. Percentages were calculated from total number of oocytes injected for number of fertilized oocytes and as a percentage of each previous category for all other categories.
[a,b] Different superscripts within columns indicate significant differences between treatments ($P < 0.05$).
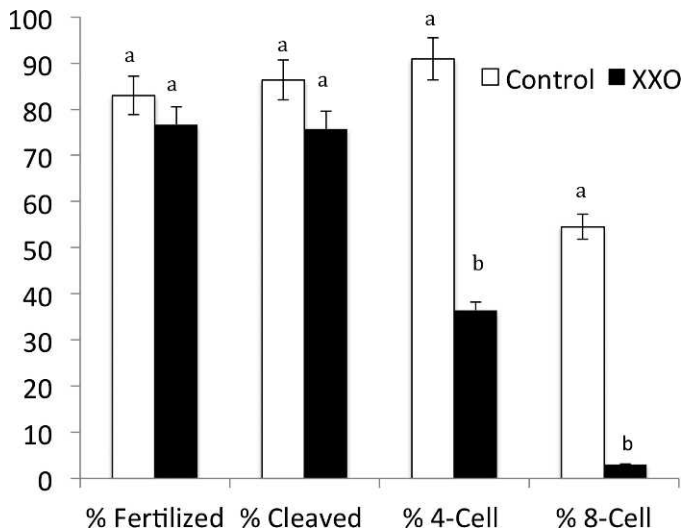
FIG. 3. Development of rhesus ICSI embryos derived from untreated fresh sperm or XXO-treated sperm through Day 3 of in vitro culture. Different superscripts indicate significant differences ($P < 0.05$).

Figure 8b depicts a four-cell embryo with normal distribution of cytoplasmic α-tubulin but with substantial nuclear fragmentation of all blastomeres present.

Transcriptome Analysis of Two-Cell Embryos Produced with ROS-Treated Sperm

Transcript abundance in two-cell embryos produced from treated and control sperm was determined using RNA-Seq. Analysis of the RNA isolated from two groups of two-cell embryos by microfluidic chip electrophoresis (Experion; BioRad) indicated an average yield of 293 pg of total RNA per embryo. Sequencing of the resultant libraries on the Illumina GAIIx platform generated a total of 74 357 197 reads that passed quality testing. Of those, 42 547 586 reads (57%) mapped to currently annotated rhesus monkey genes, and these were used to calculate the level of expression per individual transcript. A total of 8998 genes were detected as present in both samples (reads per kilobase per million > 0.3) and the correlation of reads per kilobase per million values between them was high ($r = 0.987$), indicating high similarity in global gene expression levels. Oocyte-specific genes like FIGLA, DAZL, ZP1, ZP2, MOS, NPM2, ZAR1, and H1FOO were among the expressed genes, indicating the maternal origin of transcripts at the two-cell embryo stage. Differential expression analysis was performed using DESeq, which allows for comparison of unreplicated treatments based on a negative binomial distribution, and found that there were 40 genes differentially expressed (adjusted $P < 0.05$) between treated and control samples (Supplemental Table S1, available online at www.biolreprod.org). Among differentially expressed genes, 24 and 16 were upregulated and downregulated in treated versus control embryos, respectively. Transcripts that decreased in abundance included genes related to actin cytoskeleton organization (RND3, CALD1, and FLNB) and cell junction assembly and organization (GJA1, FN1, RND3, CDH18, PCDHB4, FN1). Among upregulated genes, the only enriched biological function was related to protein amino acid phosphorylation (STK35, PDGFRA, NEK11; Table 2).

DISCUSSION

Our data provide compelling evidence that sperm subjected to high levels of oxidative stress negatively influence the developmental potential of the embryos they fertilize. The sperm we selected for ICSI in this study are not unlike those selected for clinical ICSI programs in couples with male factor infertility with regard to oxidative stress, motility, and viability characteristics. Possible mechanisms for sperm damage to impact embryo development include DNA damage to sperm; lipid peroxidation of plasma, mitochondrial, or organelle membranes; and oxidative centrosomal damage. There is also the possibility that highly oxidized sperm passively carry ROS into the egg cytoplasm at the time of sperm injection. This is not likely because injected sperm are washed extensively prior to injection. Several studies have demonstrated that sperm damage, particularly to DNA, may have adverse effects on embryo developmental and pregnancy rates [15, 49, 55, 56]. Mitotic arrest and blastomere fragmentation of our treatment group embryos correspond to reports of fragmented human embryos with aneuploidies [35, 57] and apoptosis correlated with poor embryo quality [49, 58]. Culture of embryos at atmospheric oxygen tension has been associated with increased ROS production and impaired development [59, 60]. Early cleavage divisions may be delayed, indicating a detrimental mitotic influence from ROS that later could be associated with fetal wastage and decreased fetal weight [61]. Interestingly, oxygen consumption in bovine zygotes was demonstrated to be elevated near the time of fertilization and the first cleavage division, which suggests a physiological role for ROS during preimplantation embryo development [62]. These results
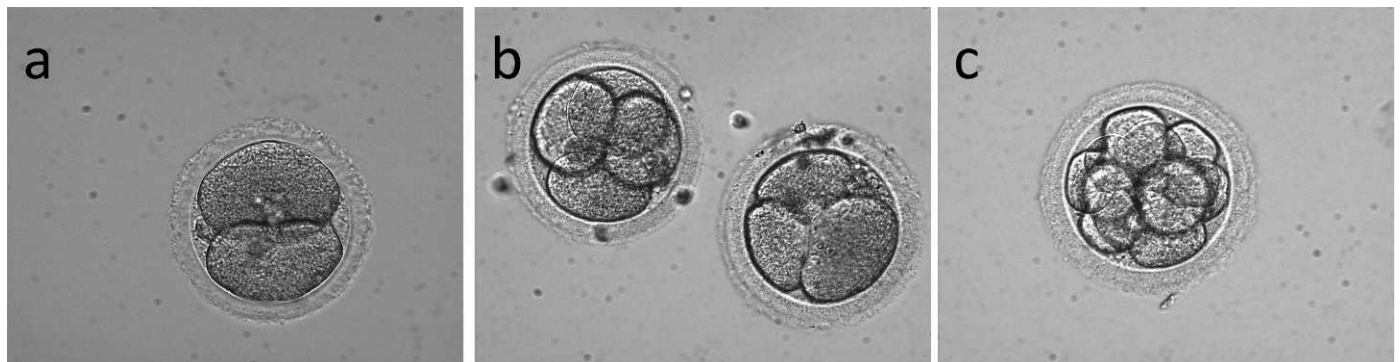

FIG. 4. Representative Hoffman modulation contrast images of rhesus macaque embryos of control sperm treatment. **a**) Two-cell embryo at 24 h post-ICSI fertilization. **b**) Two four-cell embryos at Day 2 following ICSI. **c**) Representative eight-cell embryo on Day 3 following ICSI. Note little cellular fragmentation, blastomeres filling the space inside the zona pellucida, and overall uniform cytoplasmic granularity. Original magnification ×400.
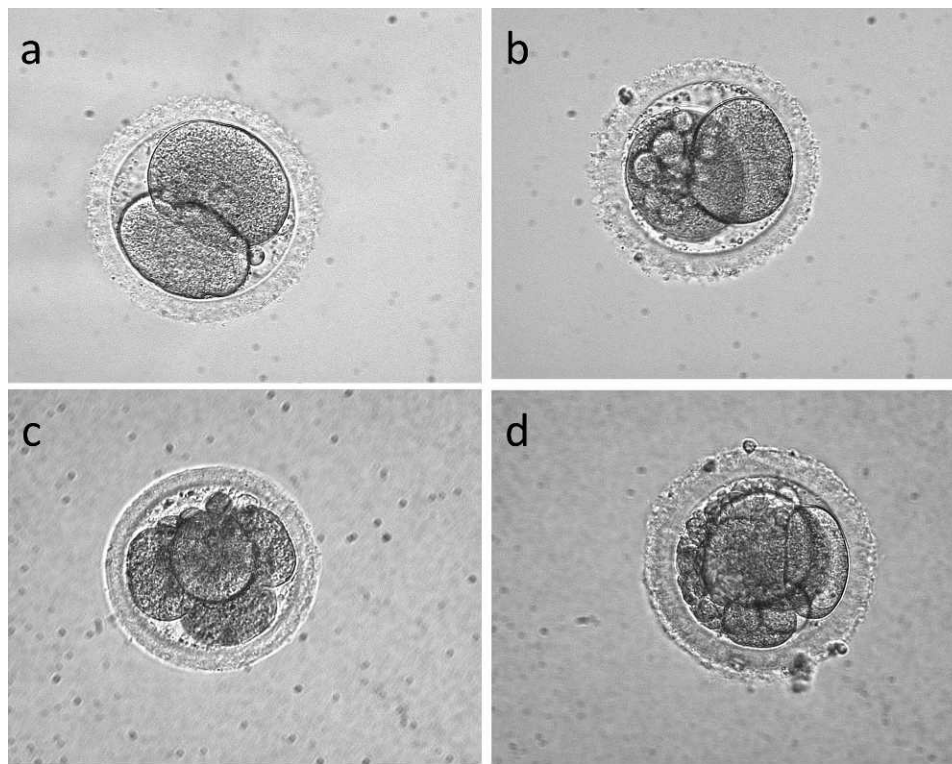
FIG. 5. Representative Hoffman modulation contrast images of rhesus macaque embryos of XXO-treated sperm. **a**) Normal-appearing two-cell embryo. **b**) Two-cell embryo with moderate amounts of blastomere fragmentation. **c**) Four-cell embryo with a few small fragments and demonstrating blastomeres not filling intrazonal space. **d**) Three-cell embryo at Day 2 with extensive fragmentation. Original magnification ×400.

suggest a particular sensitivity to ROS in the oocyte and very early developing embryo.

The concentrations of xanthine and xanthine oxidase used in this study were used by previous studies in which motile, albeit weakly, and viable spermatozoa were generated [36]. Treat-
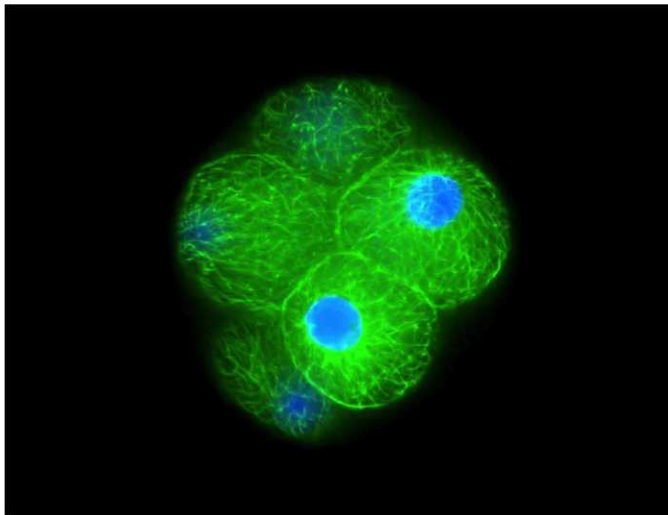

FIG. 6. Fluorescence staining of a typical eight-cell rhesus embryo from control sperm treatment group stained for α-tubulin (monoclonal anti-α-tubulin-FITC antibody) and Hoechst 3342 nuclear stain. Note uniform blastomere shape and size, intact and well-defined nuclei, and uniform distribution of α-tubulin microfilaments. Embryos were imaged at ×40 magnification using a Zeiss fluorescence microscope (AxioImager, AX10) equipped with an X-Cite Series 120 lamp and motor-driven stage for z-series sequences. Zeiss AxioVision software was used for multichannel and z-series photos. Original magnification ×400.

ment of sperm using these concentrations elicited a demonstrable embryonic effect when embryos were produced with ICSI. The treatment group embryos produced in this study exhibited severe fragmentation, multinucleation, and cell arrest well before the eight-cell stage but predominantly at the four-cell stage. Few embryos of normal morphology were observed in the treatment group beyond the two-cell stage. Aneuploid human embryos display both blastomere and nuclear fragmentation and present micronuclei [35]. In our study, embryo arrest appears to be at the two- to four-cell stage because two-celled embryos appear to have largely normal blastomeres, although low-grade blastomere cytoplasmic and nuclear fragmentation was observed.

Because of the decrease in progressive motility in our sperm following treatment, we chose to use ICSI to fertilize oocytes and produce embryos rather than in vitro fertilization. Interestingly, we found that fertilization, pronuclear formation, and first cleavage were high in the ROS-treated sperm group and not significantly different from those of controls.

Kodama and coworkers [63] observed an increase in fertilization (30%–50%) with IVF in the mouse when sperm were treated with small concentrations of Fe^{2+}/ascorbate, which are components of our ROS generating system. Their hypothesis was that the sperm membrane was modified by lipid peroxidation, rendering increased sperm fertilizing capability. However, in a bovine IVF model, a 50% decrease in fertilization was seen after sperm were exposed to high levels of ROS [64, 65]. This could indicate a species-specific difference in effect. The high rate of fertilization in our ROS treatment group (76.7%) could be representative despite lipid peroxidative damage to the sperm membrane, because the membrane must be broken to ensure fertilization with ICSI [66].
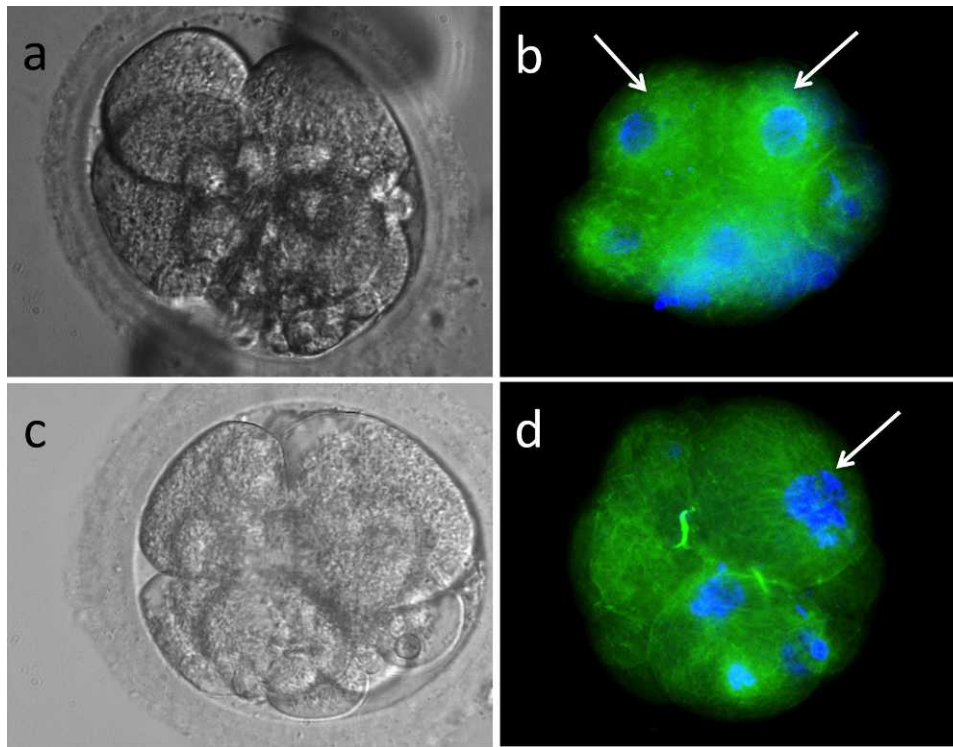
FIG. 7.   Fluorescence staining of four-cell rhesus embryos from XXO-treated sperm treatment group stained for α-tubulin (monoclonal anti-α-tubulin-FITC antibody) and Hoescht 33342 nuclear stain. **a**) Hoffman modulation contrast image of a four-cell embryo. **b**) Fluorescence image of same embryo shown in **a**. Note severe cellular fragmentation of DNA-containing fragmented cells; two blastomeres appear normal (arrows). **c**) Hoffman modulation contrast image of a four-cell fragmenting embryo demonstrating cellular debris and uneven-sized blastomeres. **d**) Fluorescence image of same embryo demonstrating several blastomeres without detectable DNA, fragmenting nuclei (arrow), and cell fragments containing DNA. Original magnification ×400.
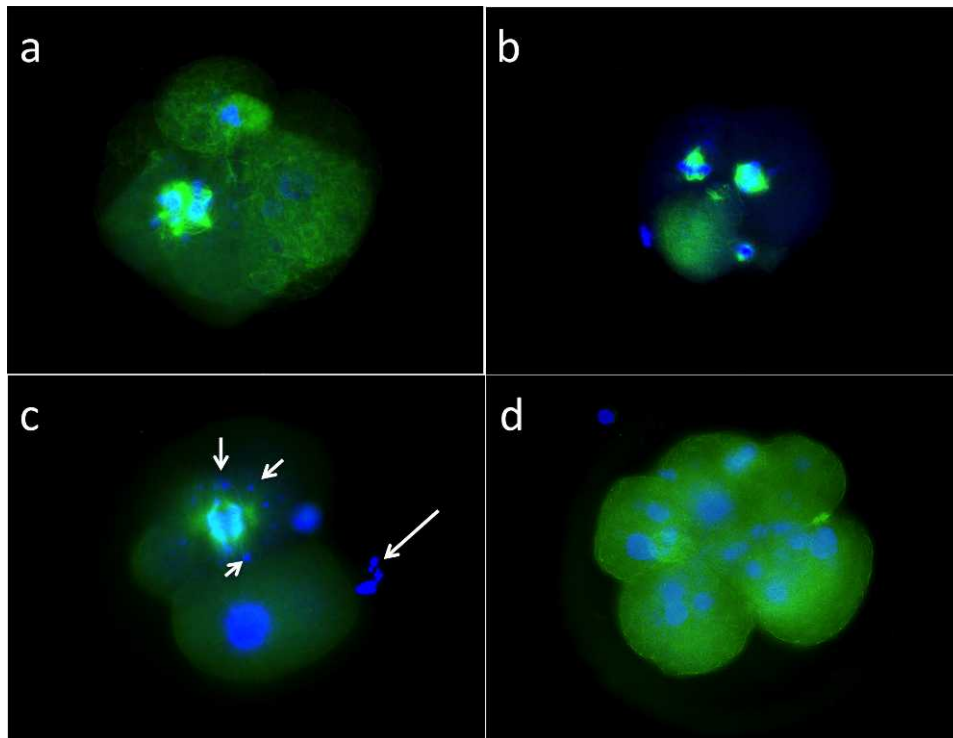
FIG. 8.   Fluorescence staining of four-cell rhesus embryos from XXO-treated sperm treatment group stained for α-tubulin (monoclonal anti-α-tubulin-FITC antibody) and Hoescht 33342 nuclear stain. **a**) Aberrant mitotic spindle. **b**) Abnormal mitotic spindles. **c**) Four-cell embryo displaying large mitotic spindle with satellite DNA fragments (small arrows); large arrow depicts fragmenting DNA associated with polar body. **d**) Fragmented DNA associated with unfragmented cytoplasm of five-cell embryo. Original magnification ×400.

Article 72

TABLE 2. Gene Ontology Biological Processes enriched in differentially expressed genes.*

Biological process	P value	Genes
Downregulated genes		
Actin cytoskeleton organization	0.036	RND3, CALD1, FLNB
Cell junction assembly	0.053	GJA1, FN1
Cell adhesion	0.063	RND3, CDH18, PCDHB4, FN1
Upregulated genes		
Protein amino acid phosphorylation	0.084	STK35, PDGFRA, NEK11

* Genes differentially expressed (adjusted $P < 0.05$) between two-cell embryos produced with control and ROS-treated sperm based on RNA-seq data were evaluated for Gene Ontology Biological Process overrepresentation using DAVID.

Sperm DNA fragmentation is associated with embryonic arrest, apoptosis, cell death, and aneuploidy resulting in low implantation and low pregnancy rates in humans [35, 56, 67, 68]. In this study, we did not assess sperm for DNA fragmentation, although other studies have demonstrated that cryopreservation and associated oxidative damage usually results in DNA fragmentation damage [6, 7]. However, embryos resulting from XXO-treated sperm did complete pronuclear development and the first two to three cleavages. This observation is similar to that seen in the bovine model when sperm damage was induced with low levels of radiation. Fatehi and coworkers [69] demonstrated that the bovine paternal genome may not be involved in the first two cleavages, but could block cleavage and development to the blastocyst stage by inducing apoptosis. Sperm DNA damage in this case, did not appear to influence bovine fertilization or the first two to three cleavages, but embryos at the four- to eight-cell stage were affected when embryonic gene transcription was activated [69]. In contrast, it has been shown that murine sperm DNA fragmentation can persist into the embryo at first cleavage and that not all fragmented DNA is repaired [70]. It is unclear whether the embryo fragmentation and embryonic arrest seen in our study is the result of sperm DNA damage. However, sperm in our study were incubated only for approximately 2 h with the XXO system, rather than overnight as in other studies, and it is possible that ROS-treated sperm did not have time to induce DNA damage. We did not examine the embryos for apoptosis but did observe abnormal spindles and nuclear fragmentation by staining embryos with α-tubulin and DAPI.

Any role of the paternal genome on subsequent embryo development is poorly understood. However, the role of sperm in activating mature oocytes and providing the zygote's centriole in nonrodent species is well known [71, 72]. The sperm centrosome has a very important role in the first mitotic cleavage and damaged or abnormal centrosomes can lead to failure of the first cleavage. Unlike the well-characterized murine fertilization system, in cattle, humans, and primates the embryonic centrosome is inherited from the sperm and thus microtubule organization after fertilization is solely the responsibility of the fertilizing sperm [72]. The centriole is an integral part of centrosomes that are in turn responsible for organizing the sperm aster and mitotic spindles in a network of microtubules. Sperm aster formation is required for pronuclear migration and union of male and female PN. Correct spindle formation allows for the correct segregation of chromosomes during mitosis. Damaged centrosomes can result in abnormal sperm asters and abnormal spindles, leading to malsegregation of chromosome and mitotic failures [72, 73]. Altered spindle

conformation leads to aneuploidy and embryonic arrest in the rhesus macaque [74]. Interestingly, in our study, rhesus sperm were predominantly labeled with C_{11}-BODIPY in the midpiece area, demonstrating significant lipid peroxidation. This is also the cellular region where the centrosome and mitochondria are located. Mitochondria and microtubules are directly involved in flagellar movement. High degrees of damage of lipid membrane peroxidation affect motility, but the exact mechanism remains unclear. It is tempting to speculate that oxidative damage to the centrosome specifically could carry over to result in abnormal cell divisions after the initial cleavage event.

Cytoplasmic fragmentation is commonly seen in all stages of human embryos produced by assisted reproductive techniques and is characterized as a morphological marker correlated to apoptosis and cell necrosis [58], abnormalities of polarity [75], aneuploidy [49, 58], and mitotic defects [35, 57]. The cause of fragmentation in human embryos is unknown. Embryos with severe and persistent fragmentation are less likely to be viable, and severe fragments observed at the one- to two-cell stage are fatal [75], whereas small amounts of fragmentation do not correlate with negative outcomes [76]. The common practice of assigning grades to embryos is based largely on blastomere fragmentation, and poor embryo grades are strongly associated with lowered implantation and pregnancy rates. In this study, fragmentation began at the first cleavage and blastomere formation was asymmetrical beginning with first cleavage similarly to that seen in human embryos [77].

The appearance of apoptotic markers and apoptotic morphological characteristics increases at the time of embryonic genomic activation and appear at the eight-cell stage rather than earlier cleavage stages in human embryos [78–80]. Apoptosis is characterized by the presence of nuclear fragmentation, cytoplasmic fragmentation, and DNA fragmentation and is associated with embryonic arrest and cell death. Although there is a strong correlation between apoptosis and fragmentation the mechanism(s) involved that link them together have not been clearly established in very early cleavage-stage embryos [33]. If the early embryo is undergoing apoptosis, it is the maternal transcription most likely driving the apoptosis, because paternal DNA is not transcriptionally active prior to EGA [80]. Some of the embryos in this study have severe fragmentation starting as early as the first cleavage. Therefore it is possible that in our experiment fragmentation, cell arrest, and possibly premature induction of apoptosis are being induced by injecting oxidatively stressed sperm. Apoptosis is not usually associated with early embryonic demise but this possibility cannot be ruled out [33, 49, 78].

Multinucleated blastomeres were also observed at Day 2 in our study. Multinucleation arises from unevenly cleaved embryos [67] and is associated with decreased implantation rates [81–84], increased chromosome abnormalities [67, 85, 86], and spontaneous abortion [87]. This is thought to occur because of problems in cytokinesis that can result in aneuploidy and disorganized embryos in humans [72, 88].

Interestingly, although the two-cell embryos appeared morphologically normal prior to arrest, the RNA-Seq analysis identified transcript abundance differences between treated and control groups. EGA in the rhesus macaque occurs at the six- to eight-cell stage [89]. Therefore, although some levels of active transcription cannot be discarded, differences in gene expression between treated and control two-cell embryos are likely to arise from changes in maternal RNA stability, translation, or degradation. For instance, an increase in transcript abundance in the embryos produced using ROS-treated sperm could be interpreted as a decrease in protein synthesis, leading to lower

mRNA degradation and accumulation of those transcripts. Also, decreased mRNA abundance could be interpreted as a higher demand for that gene's protein product, resulting in increased protein production and decreased mRNA abundance. In this study, only 40 genes were differentially expressed between treatments, which is a small number taking into consideration that almost 9000 genes were detected in these embryos. One has to consider that only one sample pool was analyzed for each condition, which is known to limit the experimental power to detect statistical differences; therefore, the current results should not be considered an exhaustive list of affected transcripts. Nevertheless, these data provide evidence that changes in mRNA abundance can be observed in cleavage stage embryos when ROS-treated sperm is used for fertilizing MII oocytes. Among genes downregulated in treated embryos, there were several involved in cytoskeletal function and cell-cell communication, such as GJA1, FN1, RND3, CDH18, PCDHB4, and FN1. This result may explain some of the morphological abnormalities later observed in these embryos, which could respond to higher demands for cytoskeletal proteins required to accommodate an oxidatively damaged sperm. GJA1 (also known as connexin 43) was 46-fold lower in treated as compared to control embryos. In mice, GJA1 depletion in the oocyte leads to abnormalities in early embryo development [90]. Interestingly, the Rho family GTPase3 (RND3), a gene altered in our study, has been reportedly affected by embryo cryopreservation in mice [91] and rabbits [92]. Because cryopreservation also induces ROS damage, it is possible that similar mechanisms lead to alterations in gene expression induced by sperm and embryo oxidative stress.

Among other genes downregulated in the treated embryos was CTCF, a zinc finger transcription factor, which was almost depleted in the treated embryos. In mice, reduction of CTCF transcript levels in oocytes and preimplantation embryos leads to altered EGA, mitotic defects, and embryo death by apoptosis [93, 94], changes similar to what was observed in this study. Unregulated genes included DHX16, a DEAH (Asp-Glu-Ala-His) box-containing helicase that in zebrafish is a maternal gene important for activation of the embryonic genome. Overall, the changes in transcript abundance observed in embryos produced from ROS-treated sperm seem to reflect the morphological abnormalities observed in these embryos and may explain the incapacity of them to undergo EGA and continued development.

Successful fertilization and subsequent embryo development are clearly dependent on oocyte structure and function. In this study, we produced embryos in a relevant model of human disease from sperm that were representative of the type of sperm damage that may result from sperm processing and environmental exposure to high levels of oxidants. Although we cannot determine the mechanism for developmental arrest in rhesus embryos in this study, we expect that further studies will elucidate the specific points in early development that paternal influences can affect embryo survival by way of oxidative membrane stress, DNA damage, centrosomal abnormalities, and aberrant gene expression.

ACKNOWLEDGMENT

REFERENCES

1. Meyers S. Cryostorage and oxidative stress in mammalian spermatozoa. In: Agarwal AAJ, Alvarez J (eds.), Studies on Men's Health and Fertility, Oxidative Stress in Applied Basic Research and Clinical Practice. New York: Springer; 2012: 41–56.
2. Aitken RJ. The role of free oxygen radicals and sperm function. Int J Androl 1989; 12:95–97.
3. Aitken RJ, Baker MA, De Iuliis GN, Nixon B. New insights into sperm physiology and pathology. Handb Exp Pharmacol 2010; 198:99–115.
4. Aitken RJ, Curry BJ. Redox regulation of human sperm function: from the physiological control of sperm capacitation to the etiology of infertility and DNA damage in the germ line. Antioxid Redox Signal 2011; 14: 367–381.
5. Baumber J, Sabeur K, Vo A, Ball BA. Reactive oxygen species promote tyrosine phosphorylation and capacitation in equine spermatozoa. Theriogenology 2003; 60:1239–1247.
6. Gandini L, Lombardo F, Lenzi A, Spano M, Dondero F. Cryopreservation and sperm DNA integrity. Cell Tissue Bank 2006; 7:91–98.
7. Li MW, Meyers S, Tollner TL, Overstreet JW. Damage to chromosomes and DNA of rhesus monkey sperm following cryopreservation. J Androl 2007; 28:493–501.
8. Toro E, Fernandez S, Colomar A, Casanovas A, Alvarez JG, Lopez-Teijon M, Velilla E. Processing of semen can result in increased sperm DNA fragmentation. Fertil Steril 2009; 92:2109–2112.
9. Baker MA, Witherdin R, Hetherington L, Cunningham-Smith K, Aitken RJ. Identification of post-translational modifications that occur during sperm maturation using difference in two-dimensional gel electrophoresis. Proteomics 2005; 5:1003–1012.
10. Aziz N, Sharma RK, Mahfouz R, Jha R, Agarwal A. Association of sperm morphology and the sperm deformity index (SDI) with poly (ADP-ribose) polymerase (PARP) cleavage inhibition. Fertil Steril 2011; 95:2481–2484.
11. Fraczek M, Sanocka D, Kurpisz M. Interaction between leucocytes and human spermatozoa influencing reactive oxygen intermediates release. Int J Androl 2004; 27:69–75.
12. Lemkecher T, Dartigues S, Vaysse J, Kulski O, Barraud-Lange V, Gattegno L, Wolf JP. Leucocytospermia, oxidative stress and male fertility: facts and hypotheses [in French]. Gynecol Obstet Fertil 2005; 33: 2–10.
13. Hammadeh ME, Radwan M, Al-Hasani S, Micu R, Rosenbaum P, Lorenz M, Schmidt W. Comparison of reactive oxygen species concentration in seminal plasma and semen parameters in partners of pregnant and non-pregnant patients after IVF/ICSI. Reprod Biomed Online 2006; 13: 696–706.
14. Zorn B, Vidmar G, Meden-Vrtovec H. Seminal reactive oxygen species as predictors of fertilization, embryo quality and pregnancy rates after conventional in vitro fertilization and intracytoplasmic sperm injection. Int J Androl 2003; 26:279–285.
15. Ahmadi A, Ng SC. Fertilizing ability of DNA-damaged spermatozoa. J Exp Zool 1999; 284:696–704.
16. Cho C, Jung-Ha H, Willis WD, Goulding EH, Stein P, Xu Z, Schultz RM, Hecht NB, Eddy EM. Protamine 2 deficiency leads to sperm DNA damage and embryo death in mice. Biol Reprod 2003; 69:211–217.
17. Evenson DP, Jost LK, Marshall D, Zinaman MJ, Clegg E, Purvis K, de Angelis P, Claussen OP. Utility of the sperm chromatin structure assay as a diagnostic and prognostic tool in the human fertility clinic. Hum Reprod 1999; 14:1039–1049.
18. Zini A, Kamal K, Phang D, Willis J, Jarvi K. Biologic variability of sperm DNA denaturation in infertile men. Urology 2001; 58:258–261.
19. Irvine DS, Twigg JP, Gordon EL, Fulton N, Milne PA, Aitken RJ. DNA integrity in human spermatozoa: relationships with semen quality. J Androl 2000; 21:33–44.
20. Wehbi E, Meriano J, Laskin C, Jarvi KA. Adverse IVF/ICSI outcomes associated with higher levels of sperm DNA fragmentation. J Urol 2009; 181:688–688.
21. Gomez E, Irvine DS, Aitken RJ. Evaluation of a spectrophotometric assay for the measurement of malondialdehyde and 4-hydroxyalkenals in human spermatozoa: relationships with semen quality and sperm function. Int J Androl 1998; 21:81–94.
22. Ollero M, Gil-Guzman E, Lopez MC, Sharma RK, Agarwal A, Larson K, Evenson D, Thomas AJ Jr, Alvarez JG. Characterization of subsets of human spermatozoa at different stages of maturation: implications in the diagnosis and treatment of male infertility. Hum Reprod 2001; 16: 1912–1921.
23. Gil-Guzman E, Ollero M, Lopez MC, Sharma RK, Alvarez JG, Thomas AJ Jr, Agarwal A. Differential production of reactive oxygen species by

subsets of human spermatozoa at different stages of maturation. Hum Reprod 2001; 16:1922–1930.

24. Ochsendorf FR. Infections in the male genital tract and reactive oxygen species. Hum Reprod Update 1999; 5:399–420.

25. Pasqualotto FF, Sharma RK, Potts JM, Nelson DR, Thomas AJ, Agarwal A. Seminal oxidative stress in patients with chronic prostatitis. Urology 2000; 55:881–885.

26. Rodriguez-Zas SL, Ko Y, Adams HA, Southey BR. Advancing the understanding of the embryo transcriptome co-regulation using meta-, functional, and gene network analysis tools. Reproduction 2008; 135: 213–224.

27. Rodriguez-Zas SL, Schellander K, Lewin HA. Biological interpretations of transcriptomic profiles in mammalian oocytes and embryos. Reproduction 2008; 135:129–139.

28. Braude P, Bolton V, Moore S. Human gene expression first occurs between the four- and eight-cell stages of preimplantation development. Nature 1988; 332:459–461.

29. Taylor DM, Ray PF, Ao A, Winston RM, Handyside AH. Paternal transcripts for glucose-6-phosphate dehydrogenase and adenosine deaminase are first detectable in the human preimplantation embryo at the three- to four-cell stage. Mol Reprod Dev 1997; 48:442–448.

30. Latham KE. The Primate Embryo Gene Expression Resource in embryology and stem cell biology. Reprod Fertil Dev 2006; 18:807–810.

31. Zheng P, Vassena R, Latham K. Expression and downregulation of WNT signaling pathway genes in rhesus monkey oocytes and embryos. Mol Reprod Dev 2006; 73:667–677.

32. Misirlioglu M, Page GP, Sagirkaya H, Kaya A, Parrish JJ, First NL, Memili E. Dynamics of global transcriptome in bovine matured oocytes and preimplantation embryos. Proc Natl Acad Sci U S A 2006; 103: 18905–18910.

33. Betts DH, Madan P. Permanent embryo arrest: molecular and cellular concepts. Mol Hum Reprod 2008; 14:445–453.

34. Xu KP, Yadav BR, Rorie RW, Plante L, Betteridge KJ, King WA. Development and viability of bovine embryos derived from oocytes matured and fertilized in vitro and co-cultured with bovine oviducal epithelial cells. J Reprod Fertil 1992; 94:33–43.

35. Chavez SL, Loewke KE, Han J, Moussavi F, Colls P, Munne S, Behr B, Reijo Pera RA. Dynamic blastomere behaviour reflects human embryo ploidy by the four-cell stage. Nat Commun 2012; 3:1251.

36. McCarthy MJ, Baumber J, Kass PH, Meyers SA. Osmotic stress induces oxidative cell damage to rhesus macaque spermatozoa. Biol Reprod 2010; 82:644–651.

37. McCarthy MJ, Meyers SA. Antioxidant treatment in the absence of exogenous lipids and proteins protects rhesus macaque sperm from cryopreservation-induced cell membrane damage. Theriogenology 2011; 76:168–176.

38. Correa LM, Thomas A, Meyers SA. The macaque sperm actin cytoskeleton reorganizes in response to osmotic stress and contributes to morphological defects and decreased motility. Biol Reprod 2007; 77: 942–953.

39. Sarason RL, VandeVoort CA, Mader DR, Overstreet JW. The use of nonmetal electrodes in electroejaculation of restrained but unanesthetized macaques. J Med Primatol 1991; 20:122–125.

40. Baumber J, Meyers SA. Changes in membrane lipid order with capacitation in rhesus macaque (Macaca mulatta) spermatozoa. J Androl 2006; 27:578–587.

41. Baumber J, Meyers SA. Hyperactivated motility in rhesus macaque (Macaca mulatta) spermatozoa. J Androl 2006; 27:459–468.

42. Aitken RJ, Buckingham D, Harkiss D. Use of a xanthine oxidase free radical generating system to investigate the cytotoxic effects of reactive oxygen species on human spermatozoa. J Reprod Fertil 1993; 97:441–450.

43. McCord JM, Fridovich I. The reduction of cytochrome c by milk xanthine oxidase. J Biol Chem 1968; 243:5753–5760.

44. World Health Organization Department of Reproductive Health and Research. WHO laboratory manual for the examination and processing of human semen. Geneva, Switzerland: World Health Organization; 2010:287.

45. Wolf DP. Assisted reproductive technologies in rhesus macaques. Reprod Biol Endocrinol 2004; 2:37.

46. Wolf DP, Thormahlen S, Ramsey C, Yeoman RR, Fanton J, Mitalipov S. Use of assisted reproductive technologies in the propagation of rhesus macaque offspring. Biol Reprod 2004; 71:486–493.

47. Meyers SA, Li MW, Enders AC, Overstreet JW. Rhesus macaque blastocysts resulting from intracytoplasmic sperm injection of vacuum-dried spermatozoa. J Med Primatol 2009; 38:310–317.

48. Schramm RD, Bavister BD. Development of in-vitro-fertilized primate embryos into blastocysts in a chemically defined, protein-free culture medium. Hum Reprod 1996; 11:1690–1697.

49. Hardy K, Stark J, Winston R. Maintenance of the inner cell mass in human blastocysts from fragmented embryos. Biol Reprod 2003; 68:1165–1169.

50. Bolton VN, Hawes SM, Taylor CT, Parsons JH. Development of spare human preimplantation embryos in vitro: an analysis of the correlations among gross morphology, cleavage rates, and development to the blastocyst. J In Vitro Fert Embryo Transf 1989; 6:30–35.

51. Head SR, Komori HK, Hart GT, Shimashita J, Schaffer L, Salomon DR, Ordoukhanian PT. Method for improved Illumina sequencing library preparation using NuGEN Ovation RNA-Seq System. Biotechniques 2011; 50:177–180.

52. Anders S, Huber W. Differential expression analysis for sequence count data. Genome Biol 2010; 11:R106.

53. Huang DW, Sherman BT, Lempicki RA. Systematic and integrative analysis of large gene lists using DAVID bioinformatics resources. Nat Protoc 2009; 4:44–57.

54. Huang DW, Sherman BT, Lempicki RA. Bioinformatics enrichment tools: paths toward the comprehensive functional analysis of large gene lists. Nucleic Acids Res 2009; 37:1–13.

55. Simon L, Proutski I, Stevenson M, Jennings D, McManus J, Lutton D, Lewis SE. Sperm DNA damage has a negative association with live-birth rates after IVF. Reprod Biomed Online 2013; 26:68–78.

56. Zini A, Libman J. Sperm DNA damage: clinical significance in the era of assisted reproduction. CMAJ 2006; 175:495–500.

57. Niakan KK, Han J, Pedersen RA, Simon C, Pera RA. Human pre-implantation embryo development. Development 2012; 139:829–841.

58. Hardy K. Apoptosis in the human embryo. Rev Reprod 1999; 4:125–134.

59. Guerin P, El Mouatassim S, Menezo Y. Oxidative stress and protection against reactive oxygen species in the pre-implantation embryo and its surroundings. Hum Reprod Update 2001; 7:175–189.

60. Kitagawa Y, Suzuki K, Yoneda A, Watanabe T. Effects of oxygen concentration and antioxidants on the in vitro developmental ability, production of reactive oxygen species (ROS), and DNA fragmentation in porcine embryos. Theriogenology 2004; 62:1186–1197.

61. Feil D, Lane M, Roberts CT, Kelley RL, Edwards LJ, Thompson JG, Kind KL. Effect of culturing mouse embryos under different oxygen concentrations on subsequent fetal and placental development. J Physiol 2006; 572:87–96.

62. Lopes AS, Lane M, Thompson JG. Oxygen consumption and ROS production are increased at the time of fertilization and cell cleavage in bovine zygotes. Hum Reprod 2010; 25:2762–2773.

63. Kodama H, Yamaguchi R, Fukuda J, Kasai H, Tanaka T. Increased oxidative deoxyribonucleic acid damage in the spermatozoa of infertile male patients. Fertil Steril 1997; 68:519–524.

64. Silva PF, Gadella BM, Colenbrander B, Roelen BA. Exposure of bovine sperm to pro-oxidants impairs the developmental competence of the embryo after the first cleavage. Theriogenology 2007; 67:609–619.

65. Hendricks KE, Penfold LM, Evenson DP, Kaproth MT, Hansen PJ. Effects of airport screening X-irradiation on bovine sperm chromatin integrity and embryo development. Theriogenology 2010; 73:267–272.

66. Kimura Y, Yanagimachi R. Intracytoplasmic sperm injection in the mouse. Biol Reprod 1995; 52:709–720.

67. Hardarson T, Hanson C, Sjogren A, Lundin K. Human embryos with unevenly sized blastomeres have lower pregnancy and implantation rates: indications for aneuploidy and multinucleation. Hum Reprod 2001; 16: 313–318.

68. Tesarik J, Greco E, Mendoza C. Late, but not early, paternal effect on human embryo development is related to sperm DNA fragmentation. Hum Reprod 2004; 19:611–615.

69. Fatehi AN, Bevers MM, Schoevers E, Roelen BA, Colenbrander B, Gadella BM. DNA damage in bovine sperm does not block fertilization and early embryonic development but induces apoptosis after the first cleavages. J Androl 2006; 27:176–188.

70. Yamauchi Y, Riel JM, Ward MA. Paternal DNA damage resulting from various sperm treatments persists after fertilization and is similar before and after DNA replication. J Androl 2012; 33:229–238.

71. Palermo GD, Colombero LT, Rosenwaks Z. The human sperm centrosome is responsible for normal syngamy and early embryonic development. Rev Reprod 1997; 2:19–27.

72. Chatzimeletiou K, Morrison EE, Prapas N, Prapas Y, Handyside AH. The centrosome and early embryogenesis: clinical insights. Reprod Biomed Online 2008; 16:485–491.

73. Sathananthan AH. Mitosis in the human embryo: the vital role of the sperm centrosome (centriole). Histol Histopathol 1997; 12:827–856.

74. Simerly C, Dominko T, Navara C, Payne C, Capuano S, Gosman G, Chong KY, Takahashi D, Chace C, Compton D, Hewitson L, Schatten G.

Molecular correlates of primate nuclear transfer failures. Science 2003; 300:297.

75. Antczak M, Van Blerkom J. Temporal and spatial aspects of fragmentation in early human embryos: possible effects on developmental competence and association with the differential elimination of regulatory proteins from polarized domains. Hum Reprod 1999; 14:429–447.

76. Racowsky C. High rates of embryonic loss, yet high incidence of multiple births in human ART: is this paradoxical? Theriogenology 2002; 57: 87–96.

77. Prados FJ, Debrock S, Lemmen JG, Agerholm I. The cleavage stage embryo. Hum Reprod 2012; 27(suppl 1):i50–i71.

78. Hardy K, Spanos S, Becker D, Iannelli P, Winston RM, Stark J. From cell death to embryo arrest: mathematical models of human preimplantation embryo development. Proc Natl Acad Sci U S A 2001; 98:1655–1660.

79. Spanos S, Rice S, Karagiannis P, Taylor D, Becker DL, Winston RM, Hardy K. Caspase activity and expression of cell death genes during development of human preimplantation embryos. Reproduction 2002; 124:353–363.

80. Jurisicova A, Acton BM. Deadly decisions: the role of genes regulating programmed cell death in human preimplantation embryo development. Reproduction 2004; 128:281–291.

81. Jackson KV, Ginsburg ES, Hornstein MD, Rein MS, Clarke RN. Multinucleation in normally fertilized embryos is associated with an accelerated ovulation induction response and lower implantation and pregnancy rates in in vitro fertilization-embryo transfer cycles. Fertil Steril 1998; 70:60–66.

82. Pelinck MJ, De Vos M, Dekens M, Van der Elst J, De Sutter P, Dhont M. Embryos cultured in vitro with multinucleated blastomeres have poor implantation potential in human in-vitro fertilization and intracytoplasmic sperm injection. Hum Reprod 1998; 13:960–963.

83. Van Royen E, Mangelschots K, Vercruyssen M, De Neubourg D, Valkenburg M, Ryckaert G, Gerris J. Multinucleation in cleavage stage embryos. Hum Reprod 2003; 18:1062–1069.

84. Moriwaki T, Suganuma N, Hayakawa M, Hibi H, Katsumata Y, Oguchi H, Furuhashi M. Embryo evaluation by analysing blastomere nuclei. Hum Reprod 2004; 19:152–156.

85. Agerholm IE, Hnida C, Cruger DG, Berg C, Bruun-Petersen G, Kolvraa S, Ziebe S. Nuclei size in relation to nuclear status and aneuploidy rate for 13 chromosomes in donated four cells embryos. J Assist Reprod Genet 2008; 25:95–102.

86. Pickering SJ, Taylor A, Johnson MH, Braude PR. An analysis of multinucleated blastomere formation in human embryos. Hum Reprod 1995; 10:1912–1922.

87. Scott L, Finn A, O'Leary T, McLellan S, Hill J. Morphologic parameters of early cleavage-stage embryos that correlate with fetal development and delivery: prospective and applied data for increased pregnancy rates. Hum Reprod 2007; 22:230–240.

88. Xanthopoulou L, Delhanty JD, Mania A, Mamas T, Serhal P, Sengupta SB, Mantzouratou A. The nature and origin of binucleate cells in human preimplantation embryos: relevance to placental mesenchymal dysplasia. Reprod Biomed Online 2011; 22:362–370.

89. Zheng P, Patel B, McMenamin M, Reddy SE, Paprocki AM, Schramm RD, Latham KE. The primate embryo gene expression resource: a novel resource to facilitate rapid analysis of gene expression patterns in non-human primate oocytes and preimplantation stage embryos. Biol Reprod 2004; 70:1411–1418.

90. Gershon E, Plaks V, Aharon I, Galiani D, Reizel Y, Sela-Abramovich S, Granot I, Winterhager E, Dekel N. Oocyte-directed depletion of connexin43 using the Cre-LoxP system leads to subfertility in female mice. Dev Biol 2008; 313:1–12.

91. Mamo S, Bodo S, Kobolak J, Polgar Z, Tolgyesi G, Dinnyes A. Gene expression profiles of vitrified in vivo derived 8-cell stage mouse embryos detected by high density oligonucleotide microarrays. Mol Reprod Dev 2006; 73:1380–1392.

92. Saenz-de-Juano MD, Marco-Jimenez F, Penaranda DS, Joly T, Vicente JS. Effects of slow freezing procedure on late blastocyst gene expression and survival rate in rabbit. Biol Reprod 2012; 87:91.

93. Wan LB, Pan H, Hannenhalli S, Cheng Y, Ma J, Fedoriw A, Lobanenkov V, Latham KE, Schultz RM, Bartolomei MS. Maternal depletion of CTCF reveals multiple functions during oocyte and preimplantation embryo development. Development 2008; 135:2729–2738.

94. Moore JM, Rabaia NA, Smith LE, Fagerlie S, Gurley K, Loukinov D, Disteche CM, Collins SJ, Kemp CJ, Lobanenkov VV, Filippova GN. Loss of maternal CTCF is associated with peri-implantation lethality of Ctcf null embryos. PLoS One 2012; 7:e34915.